

# 3D Finite Element Analysis of Flexible Induction Heating System of Metallic Sheets

T. Tudorache and P. Deaconescu

University POLITEHNICA of Bucharest, EPM\_NM Laboratory, Bucharest, Romania

**Abstract**— This paper deals with the finite element based numerical analysis of a flexible induction heating system used in the continuous heating lines of metallic sheets. Several field numerical models for solving the 3D electromagnetic field problem associated to the device are compared and characterized from numerical point of view. The results of the thermal field analysis of the device are validated by experimental measurements. The 3D electromagnetic and thermal field analysis of the device proves an important transversal non-uniformity of the temperature profile of the sheet that can be diminished by using special flexible magnetic structures able to screen the lateral edges of the sheet.

## I. INTRODUCTION

One of the actual technologies of electromagnetic processing of materials is the continuous induction heating of metallic sheets in transverse flux. The development and improvement of such technology, having as support especially the steel and aluminum alloys sheets, represent an objective of strategic economical importance, taking into account the major industrial impact of the use of flat metallic products in various market segments such as: wrapping and preserving of food products, containers, recipients, vessels, vehicles and equipment shells, metallic casings and shields etc.

Among the various types of inductors two types can be used to heat metallic sheets i.e. *longitudinal flux* inductors and *transverse flux* inductors. Unlike the classical *longitudinal flux* inductors, the *transverse flux* inductors consist of two or several pairs of coils mounted on two magnetic armatures, Fig. 1. The a.c. inductor field produced by the coils determines the development of eddy currents that by Joule effect increases the sheet temperature.

A major advantage of *Transverse Flux Induction Heating* (TFIH) of metallic sheets compared to *longitudinal flux* heating is represented by a higher electric efficiency at reduced frequency values that confers to this technique a promising future. However this heating technique is characterized by great difficulties in ensuring a uniform temperature transversal profile of the moving metallic sheets, [1], the amelioration of this aspect being an actual research subject representing a major priority of many recognized research teams.

## II. FINITE ELEMENT MODELS

### A. Electromagnetic field computation models

The design and optimization of TFIH systems supposes the understanding and the correlation of the electric,

magnetic, thermal and mechanical complex effects in order to control the specific technological parameters. In this context the study and analysis of such equipment requires modern numerical investigation tools the most suitable being the finite element method.

By exploiting the geometrical and physical symmetries, represented by the planes XOY, XOZ, YOZ, the computation domain of the 3D electromagnetic field associated to the TFIH system will reduce to 1/8 of the complete geometry, Fig. 2. From electromagnetic point of view the computation domain contains several types of regions with different physical properties:

- *inductor coils* (A), source of magnetic field, characterized by a current with given constant density, considered as non-magnetic and non-conducting regions;
- *magnetic cores* (B), considered as magnetic, non-conducting and no-source regions;
- *metallic sheet* (C), considered as conducting and no-source region;
- *surrounding air* (D), that have the properties of vacuum, i.e. non-magnetic, non-conducting and no-source region.

Five 3D quasi-static electromagnetic field models associated to the TFIH device will be analyzed in this paper:

a)  $T\Phi-\Phi-\Phi_{red}$  model, that represents the coupling of the  $T\Phi$  formulation, in electric vector potential  $T$  and magnetic scalar potential  $\Phi$  in region (C), with the  $\Phi$  formulation in region (B), respectively with the formulation  $\Phi_{red}$ , in reduced magnetic scalar potential, in regions (A) and (D).

a1)  $T\Phi$  formulation is characterized by the following equations expressed in potentials:

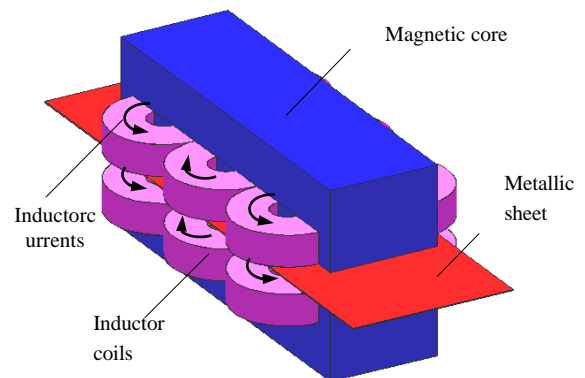


Figure 1. Transverse flux induction heating system of metallic sheets

$$\text{curl} [(1/\sigma) \text{curl} \mathbf{T}] - \nabla [(1/\sigma_p) \nabla \cdot \mathbf{T}] + j\omega\mu(\mathbf{T} - \nabla \Phi) = 0 \quad (1)$$

$$\nabla \cdot [\mu(\mathbf{T} - \nabla \Phi)] = 0, \quad (2)$$

where:  $-\nabla[(1/\sigma_p) \cdot \nabla \cdot \mathbf{T}]$  represents the penalty term used to impose the Coulomb gauge ( $\nabla \cdot \mathbf{T} = 0$ ),  $\mu$  and  $\sigma$  represents the magnetic permeability, respectively the electric conductivity of the region, and  $\omega$  the electromagnetic field pulsation.

a2)  $\Phi$  formulation is governed by the following equation:

$$\nabla \cdot [\mu(-\nabla \Phi)] = 0 \quad (3)$$

a3) In case of  $\Phi_{red}$  formulation, the source magnetic field  $\mathbf{H}_0$ , generated by the coil type regions, supplied by a current with a constant density  $J_{ex}$ , is computed using the Biot – Savart – Laplace formula. The equation associated to this formulation is:

$$\nabla \cdot [\mu_0(-\nabla \Phi_{red} + \mathbf{H}_0)] = 0, \quad (4)$$

where  $\mu_0$  represents the magnetic permeability of vacuum.

b) *AV-A model*, represented by the coupling of the *AV* formulation, in magnetic vector potential  $\mathbf{A}$  and electric scalar potential  $V$  in region (C) with *A* formulation in regions (A), (B) and (D).

b1) *AV formulation* is characterized by the following equations expressed in potentials:

$$\text{curl} [(1/\mu) \text{curl} \mathbf{A}] - \nabla [(1/\mu_p) \nabla \cdot \mathbf{A}] + \sigma(j\omega \mathbf{A} + \nabla V) = 0 \quad (5)$$

$$\nabla \cdot [\sigma(j\omega \mathbf{A} + \nabla V)] = 0, \quad (6)$$

where  $-\nabla[(1/\sigma_p) \nabla \cdot \mathbf{A}]$  represents the penalty term used to impose the Coulomb gauge ( $\nabla \cdot \mathbf{A} = 0$ ).

b2) *A formulation* is characterized by the equations:

$$\text{curl} [(1/\mu) \text{curl} \mathbf{A}] - \nabla [(1/\mu_p) \nabla \cdot \mathbf{A}] = \mathbf{J}_{ex} \quad (7)$$

c) *AV- $\Phi$ - $\Phi_{red}$  model* represented by the coupling of the *AV* formulation in region (C), with  $\Phi$  formulation in regions (B), respectively with  $\Phi_{red}$  formulation in regions (A) and (D). The equations of this model, expressed in potentials, are (5), (6), (3) and (4).

d) *Hyperb\_J\_Conductor-  $\Phi$  -  $\Phi_{red}$  model* that represents the coupling of the *Hyperb\_J\_Conductor* surface formulation implemented in FLUX3D in region (C), with  $\Phi$  formulation in regions (B), respectively with  $\Phi_{red}$  formulation in regions (A) and (D). The *Hyperb\_J\_Conductor formulation* supposes to model the metallic sheet region (C) as surface region and consists in coupling the electromagnetic field associated quantities on the two faces of the conducting region [2]. This field model supposes in FLUX3D to build the computation domain of the 3D electromagnetic field only by exploiting the symmetries associated to planes XOZ and YOZ. The resulting computation domain in this case is different from that in Fig. 2, and represents a fourth of the complete geometry.

e) *Const\_J\_Conductor - A model*, that represents the coupling of the surface formulation *Const\_J\_Conductor* in

region (C), and of *A* formulation in regions (A), (B) and (D). The surface formulation *Const\_J\_Conductor* is a formulation without potential jump and supposes the modeling of thin conducting regions by surface type regions, the condition of using the formulation being that the penetration depth of electromagnetic field to be much larger than the conducting region thickness [2].

Depending on the types of regions and formulations, the boundary conditions, Fig. 2, expressed in potentials, are as follows:

$$\partial \Phi / \partial n = 0, \quad \partial \Phi_{red} / \partial n = 0, \quad \mathbf{T} \cdot \mathbf{n} = 0, \quad \mathbf{A} \times \mathbf{n} = 0, \quad V = \text{constant}, \quad \text{on boundaries with } \mathbf{B} \cdot \mathbf{n} = 0,$$

$$\Phi = \text{constant}, \quad \Phi_{red} = \text{constant}, \quad \mathbf{T} \times \mathbf{n} = 0, \quad \mathbf{A} \cdot \mathbf{n} = 0, \quad \partial V / \partial n = 0, \quad \text{on boundaries with } \mathbf{H} \times \mathbf{n} = 0.$$

The frontier at infinite of open boundary electromagnetic field problems, as in our case, is modeled in FLUX3D by a particular region called *infinite box*, based on an inverse transformation of Kelvin type, of the real unbounded space into a bounded space, Fig. 2.

### B. Thermal field computation model

The sheet transient temperature field  $T(\mathbf{r}, t)$  satisfies the Fourier equation:

$$\rho \cdot C_p \cdot dT/dt = \nabla \cdot (k \cdot \nabla T) + pJ, \quad (8)$$

where  $k$ ,  $\rho$ ,  $C_p$  represent thermal conductivity, mass density and specific heat of the sheet respectively.

We assume that the sheet resistivity has a constant value that corresponds to the average temperature of the process that means a time independent thermal source  $pJ$ . Without this assumption at each time step a 3D magneto-thermal coupling would be necessary that leads to a prohibitively long computation time.

The initial condition,  $T(\mathbf{r}, 0) = T_0$  and the boundary conditions on the surfaces S1 ... S6, associated to (8), are presented in Fig. 3, where:  $\beta(T)$  stands for the thermal transfer coefficient from the sheet surface to the surrounding air and  $Ta$  stands for the ambient temperature.

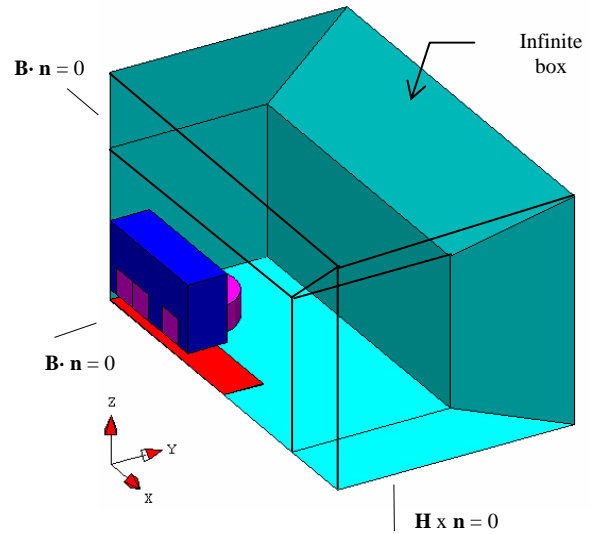


Figure 2. Electromagnetic field computation domain and boundary conditions

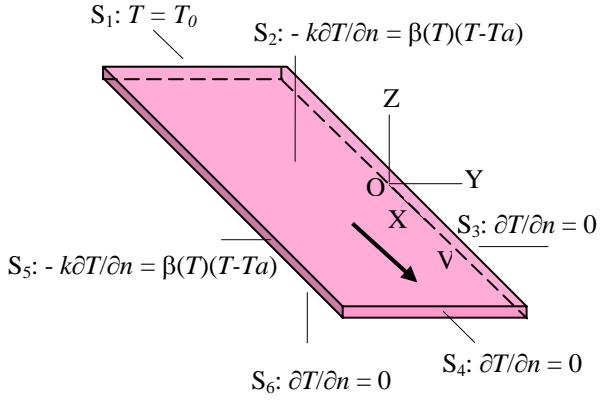


Figure 3. Thermal field computation domain and boundary conditions

The temperature on the sheet thickness  $h$  is considered invariable and therefore shell first order finite elements of rectangular shape are used for numerical integration of (8) in combination with a typical Galerkin scheme.

Starting from the initial thermal state, the sheet temperature field is calculated step by step in time, solving the matrix equation of the form:

$$[M] \cdot \frac{[T]^k - [T]^{k-1}}{\Delta t} + [A] \cdot [T]^k = [B] \quad (9)$$

The thermal field computation considers the sheet motion along the inductor air gap by a “moving mesh” scheme, [3] in the inductor referential, the nodes position changing after each time step  $\Delta t$ . The ratio between the incremental mesh displacement  $\Delta x$  and  $\Delta t$  is the sheet velocity,  $V = \Delta x / \Delta t$ .

### C. Characterization of electromagnetic field models

The characterization of the five 3D electromagnetic field models from numerical performance point of view is an important issue that takes into account the following criteria: accuracy of local and global results, number of equation and computation time. In order to keep the comparative analysis as objective as possible the field numerical models are based on the same level of mesh refinement in the computation domain regions.

The numerical applications are performed for the following data, Fig. 2: inductor length 340 mm, pole pitch length 100 mm, magnetic core width 100 mm, magnetic core relative permeability 1000, coils cross section 35 x 35 mm, inductor air gap thickness 10 mm, aluminum sheet of 1 mm thickness and 100 mm width, supply frequency 430 Hz.

The chart of the induced power density in the metallic sheet, obtained by solving the 3D electromagnetic field problem associated to the heating system and by post-processing the solution is presented in Fig. 4. This chart is characterized by a strong non-uniformity that entails a transversal non-uniformity of the temperature profile of the sheet. The transversal non-uniformity of the sheet heating is reflected very well by the transversal profile  $Profile(Y)$  of induced power density integrated along the inductor [1]. The transversal profiles, Fig. 5, obtained by using the five electromagnetic field models are very close to each other, the best one being identified and selected based on the numerical performances.

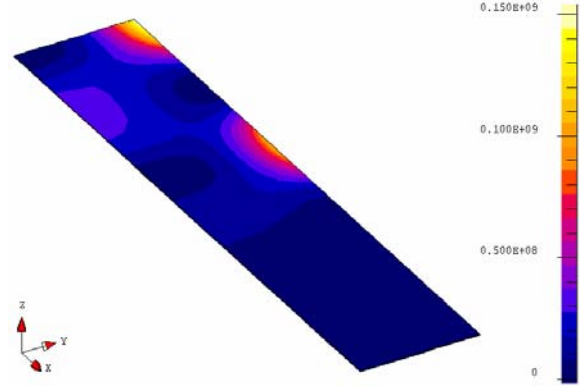


Figure 4. Induced power density chart

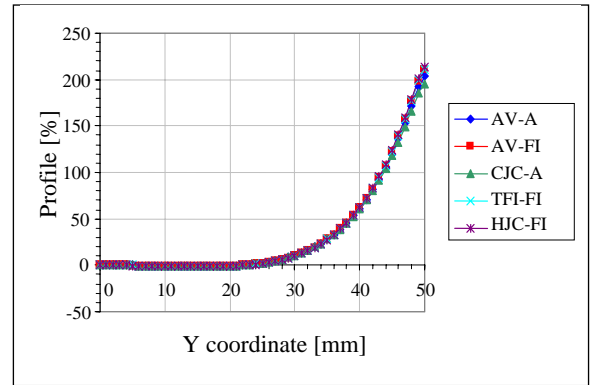


Figure 5. Transversal profile of induced power density

By the analysis of the numerical results in Table I, related to the local and global quantities obtained using FLUX3D software package: maximum value of induced current density  $J_{2max}$ , induced power  $P_2$ , maximum and minimum value  $Max_{pr}$  and  $Min_{pr}$ , of function  $Profile(Y)$ , respectively based on the numerical performances expressed by *Number of equations* and *Computation time*, we can formulate the following conclusions:

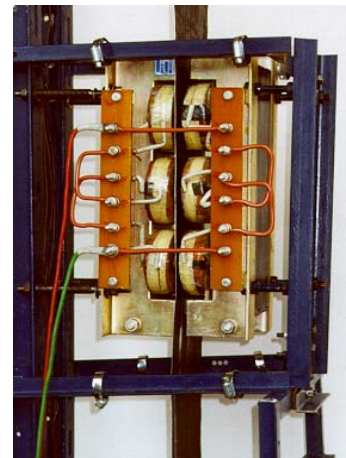


Figure 6. Experimental TFIH device

TABLE I.  
NUMERICAL RESULTS ON A PC, PENTIUM IV, 1.6 GHZ

Field model	$J_{2max}$ [A/mm <sup>2</sup> ]	$P_2$ [kW]	$Max_{pr}$ [%]	$Min_{pr}$ [%]	No. eq.	CPU time [s]
$T\Phi$ - $\Phi$ - $\Phi_{red}$	88.18	82.99	210.87	-1.24	15715	80
$HJC$ - $\Phi$ - $\Phi_{red}$	87.71	81.36	213.62	-1.34	24403	75
$AV$ - $\Phi$ - $\Phi_{red}$	88.24	82.99	210.65	-1.30	20469	97
$AV$ - $A$ - $A$	85.98	79.28	204.17	-1.16	40830	131
$CJC$ - $A$ - $A$	82.75	76.40	195.19	-1.21	34679	94

- The differences between the results of the five field models are very small;
- The  $T\Phi$ - $\Phi$ - $\Phi_{red}$  field model is the most economic in terms of equations number, and the  $Hyperb_J$ - $Conductor$ - $\Phi$ - $\Phi_{red}$  model is the most economic concerning the computation time;
- The numerical values of the results of the  $AV$ - $A$  and  $Constant_J$ - $Conductor$ - $A$  field models related to the quantities  $P_2$ ,  $J_{2max}$ ,  $Max_{pr}$ , are smaller than the values obtained by the other three field models;
- The  $AV$ - $A$  field model is the most inefficient in terms of equations number and computation time due to the presence of magnetic vector potential  $A$  in the non-conducting regions that supposes 6 unknowns per node in comparison with only 2 unknowns per node in case of  $\Phi$  and  $\Phi_{red}$  formulations [4].

### III. EXPERIMENTAL VALIDATION OF NUMERICAL RESULTS

In order to validate the numerical modeling results, two cases were studied, using the experimental facility presented in Fig. 6, the sheet material being aluminum. The laboratory experimental tests used a thermocouple based temperature measurement system.

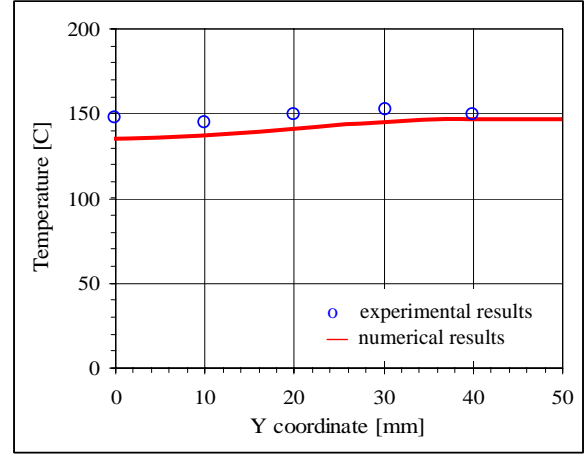
In Case 1 the metallic sheet is characterized by 1 mm thickness and 100 mm width, supply frequency 426 Hz, current per coil 385 A r.m.s and sheet velocity 0.047 m/s.

In Case 2 the metallic sheet is characterized by 1 mm thickness, 150 mm width, supply frequency 430 Hz, current per coil 385 A r.m.s., sheet velocity 0.042 m/s.

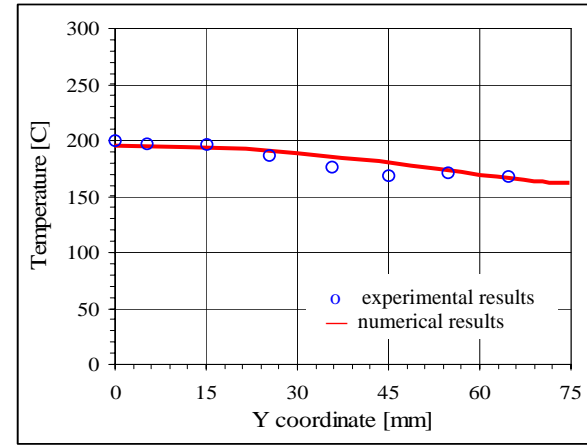
The transversal variation of the sheet temperature at the inductor exit is presented in Fig. 7 for the two studied cases.

The transversal variation of the sheet temperature at the inductor exit, Fig. 7, emphasizes a good agreement between the numerical modeling and the experimental measurement results.

The comparison between the two applications shows at sheet edges an overheating in Case 1, due to a local concentration of eddy currents, Fig. 4, respectively an under-heating in Case 2, when the sheet is larger than the magnetic core.



a)



b)

Figure 7. Transversal temperature profile a) Case 1; b) Case 2

### IV. FLEXIBLE MAGNETIC SHIELDING SYSTEM FOR THERMAL FIELD IMPROVEMENT

In case of industrial TFIH developments the sheet velocities are larger than the ones considered in the previous section. In this case, the transversal profile of the sheet temperature at the inductor outlet is influenced mainly by the induced power density integrated along the inductor, the thermal conduction having a reduced role in the thermal homogenization. Thus the conclusions drawn from the analysis of this type of profile applies also to the temperature transversal profile.

An efficient continuous heating line of industrial scale should respond to different client requirements that usually mean the capability of heating uniformly at different temperatures a wide range of sheet widths, thicknesses and materials. In this context the TFIH integrated in the industrial line should be characterized by a large degree of adaptability to the sheet characteristics.

A flexible and effective solution consists in equipping the classical TFIH device with two magnetic shields used as regulating elements of temperature transversal profile of the sheet, Fig. 8.

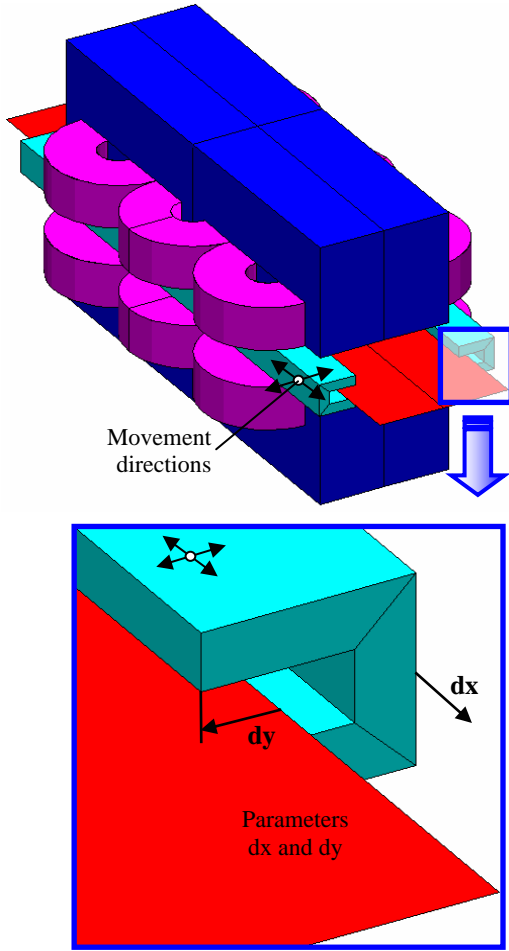


Figure 8. TFIH device equipped with magnetic shields. Orthogonal movement directions characterized by the parameters  $dx$  and  $dy$

The effect of these magnetic structures is the change of the induced currents path by shielding the sheet edges [5]. Such laminations made magnetic shields, having the  $\subset$  shape are placed around each sheet edge and have two independent movement directions, a longitudinal one and a transversal one. The simultaneous movement of the two magnetic structures along the two orthogonal directions (along OX and along OY axes) permits the tuning of the transversal profile of the metallic sheet depending on the sheet characteristics.

The study of the magnetic shielding influence on the TFIH characteristics is carried out on the Case 1 arrangement, but with an inductor air gap enlarged to 30 mm permitting the positioning of two magnetic shields of 8 mm thickness around the sheet edges.

The influence of the magnetic shields movement along the two orthogonal directions on the profile of induced power density integrated along the inductor is studied by varying the two specific geometrical parameters  $dx$  and  $dy$ , Fig. 8.

Parameter  $dx$  is used to characterize the displacement of the magnetic shields along the OX axis with respect to the center of the TFIH system. Parameter  $dy$  represents the sheet width covered by the magnetic shields, this parameter being varied by the simultaneous movement of the magnetic shields along OY axis.

The numerical results in Fig. 9, prove that both  $dx$  and  $dy$  parameters have a strong influence on the transversal profile of induced power density integrated along the inductor and may be used successfully to regulate the temperature transversal profile of the metallic sheets.

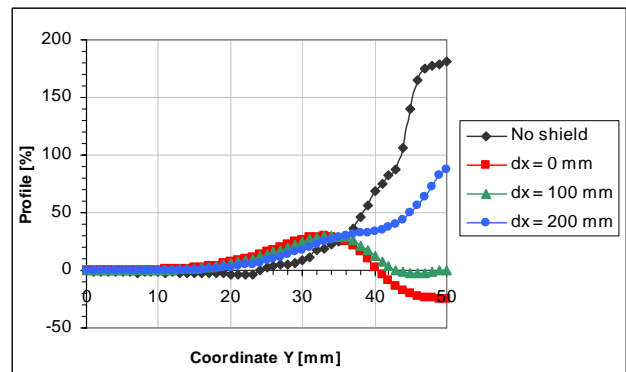
## V. CONCLUSIONS

The numerical analysis of TFIH device using different 3D electromagnetic field models proved that the *Hyperb\_J\_Conductor- $\Phi$ - $\Phi_{red}$*  and *T $\Phi$ - $\Phi$ - $\Phi_{red}$*  models are the most economic in terms of computation time and number of unknowns.

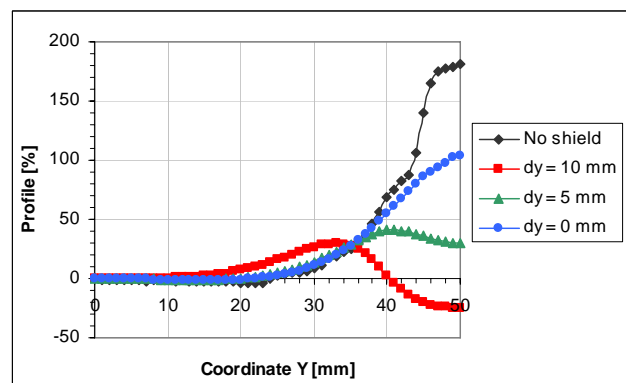
The numerical results obtained using the dedicated program developed to compute the thermal field evolution of the metallic sheet heated by the TFIH system are in good agreement with the experimental ones.

The proposed magnetic shielding system with double direction movement capability was proved to be a very efficient and flexible technical solution that can be used to improve the sheet transversal temperature uniformity of the sheet.

Further research activity should be carried out in order to find the best magnetic shields parameters by using optimization algorithms coupled with the 3D finite element model of the device.



a)



b)

Figure 9. Influence of  $dx$  and  $dy$  parameters on the transversal profile of induced power density integrated along the inductor

## ACKNOWLEDGMENT

This paper is a result of a research activity partially supported by a CEEX grant and we take this occasion to thank CNCSIS-UEFISCSU for the support.

## REFERENCES

- [1] T. Tudorache, V. Fireteanu: "3D Numerical Modeling of New Structures for Transverse Flux Heating of Metallic Sheets", *Proc. of IHS 1998*, Padova, Italy, May, 1998.
- [2] V. Fireteanu, B. Paya, J. Nuns, T. Tudorache: "Numerical Evaluation of Eddy Currents in Thin conducting Regions modeled as Surface Regions", *Proc. of COMPUMAG - TEAM Workshop and Applications Forum*, Evian, France, July, 2001.
- [3] T. Tudorache, B. Paya, J-C. Bourhis, V. Fireteanu: "Numerical Modeling and Optimization by Magnetic Shielding of Transverse Flux Induction Heating", *Proc. of IGTE 8<sup>th</sup> Symposium*, Graz, Austria, Sept., 1998.
- [4] V. Fireteanu, T. Tudorache: "Couplings of Electromagnetic Field Formulations in Finite Element Analysis of Transverse Flux Induction Heating Systems", *Proc. of ISEF 2005*, Baiona, Spain, Sept., 2005.
- [5] T. Tudorache, V. Fireteanu: "Optimization of Magnetic Screening in Transverse Flux Induction Heating", *Proc. of the 48<sup>th</sup> IWK*, Ilmenau, Germany, Sept., 2003.